HHS Public Access

Author manuscript

Genes Chromosomes Cancer. Author manuscript; available in PMC 2023 December 01.

Published in final edited form as:

Genes Chromosomes Cancer. 2022 December ; 61(12): 701–709. doi:10.1002/gcc.23083.

Recurrent *VGLL3* Fusions Define A Distinctive Subset of Spindle Cell Rhabdomyosarcoma with An Indolent Clinical Course And Striking Predilection For The Head and Neck

Abbas Agaimy, MD[1], **Josephine K. Dermawan, MD, PhD**[2], **Iona Leong, BDS, MSc**[3,4,5], **Robert Stoehr, PhD**[1], **David Swanson, BSc.**[4], **Ilan Weinreb, MD**[5,6], **Lingxin Zhang, MD**[4,5], **Cristina R. Antonescu, MD**[2], **Brendan C. Dickson, MD, MSc.**[4,5]

[1]Institute of Pathology, Erlangen University Hospital, Comprehensive Cancer Center, European Metropolitan Area Erlangen-Nuremberg (CCC ER-EMN), Friedrich Alexander University of Erlangen-Nuremberg, Erlangen, Germany

[2]Department of Pathology, Memorial Sloan Kettering Cancer Center, New York, NY, USA

[3]Faculty of Dentistry, University of Toronto, Toronto, ON, Canada

[4]Department of Pathology & Laboratory Medicine, Mount Sinai Hospital, Toronto, ON, Canada

[5]Department of Pathobiology and Laboratory Medicine, University of Toronto, Toronto, ON, Canada

[6]Laboratory Medicine Program, University Health Network, Toronto, ON, Canada

Abstract

The mammalian Vestigial-like (VGLL) transcriptional cofactor family of proteins VGLL1-4 has recently emerged as an important player in the tumorigenesis of diverse neoplasms. The role of *VGLL3* in soft tissue tumors is exemplified by its amplification in myxoinflammatory fibroblastic sarcoma and its rearrangement (fused to *CHD7, CHD9* or *MAMLD1*) in hybrid schwannoma-perineurioma. This study characterizes a distinctive low-grade myogenic neoplasm with a striking predilection for the head and neck, characterized by *VGLL3* fusions. The study includes five males and one female patient, aged 30 to 71 years (median, 56). Three tumors originated in the tongue, with one case each in the nasopharynx, oral cavity, and oropharynx. The *VGLL3* fusion partners included *TCF12* (n=3), *EP300* (n=2) and *PPARGC1A* (n=1). The tumor size range was 0.8 – 1.6 cm (all, but one, was <1cm). Histologically, all tumors displayed bland spindle to ovoid cells arranged into vague fascicular and diffuse pattern. Mitotic activity ranged from 1 to 7 per 10 HPFs. Five tumors were muscle-centered and infiltrative, and one was centered beneath nasopharyngeal mucosa. Immunohistochemistry revealed consistent expression of desmin (diffuse in four and patchy in two cases) associated with patchy smooth muscle actin expression (4/6), and focal reactivity for myogenin (5/6) and myoD1 (1/3). All patients were managed surgically; one patient each received adjuvant radio- or chemotherapy. Three patients with follow-up were

Address page proofs, correspondence, and requests for reprints to: Abbas Agaimy, MD, Pathologisches Institut, Universitätsklinikum Erlangen, Krankenhausstrasse 8-10, 91054 Erlangen, Germany, Phone: +49-9131-85-22288, Fax: +49-9131-85-24745, abbas.agaimy@uk-erlangen.de.

Conflict of interest: none

without disease at 8, 19, and 60 months and one was alive with unknown disease status at 24 months. All *VGLL3* fusions were in-frame and involved exon 2, fused with either *TCF12* exon 16, *EP300* exon 31 or *PPARGC1A* exon 5, respectively. This series characterizes a distinctive subset of spindle cell rhabdomyosarcoma with a predilection for the head and neck in adults, defined by *VGLL3* fusions, likely indolent behavior and limited rhabdomyoblastic differentiation. Further delineation of this entity and differentiation from more aggressive molecular subtypes of spindle cell rhabdomyosarcoma is mandatory to define the most appropriate therapeutic strategy and avoid overtreatment.

Keywords

Spindle cell rhabdomyosarcoma; VGLL3; head and neck; EP300; TCF12; PPARGC1A; gene fusion; sarcoma

INTRODUCTION

The mammalian Vestigial-like (VGLL) proteins are a family of TEAD-interacting transcriptional cofactor proteins, deriving their name from their similarity to the Vestigial transcriptional cofactor of the Drosophila [1–4]. To date, four mammalian VGLL proteins (VGLL1-4) have been identified [1–4], sharing similar TEAD-interacting domain (TDU), but otherwise their sequences are dissimilar [1–4].

The VGLL proteins are emerging as important players in the tumorigenesis of diverse neoplasms in different organs [4]. VGLL1 was found to be highly expressed in basal-like breast cancer, where it likely promotes cellular proliferation [5]. Moreover, in the capacity of a putative genetic driver, *VGLL2* has been recognized as fusion partner in subsets of head and neck spindle cell rhabdomyosarcomas (RMS), usually fused to *NCOA2*, *TEAD1*, *CITED2* as well as several other partners [6].

The role of *VGLL3* alterations in mesenchymal neoplasms has been limited to a few recently reported studies. Amplification of *VGLL3* (mapped to chromosome 3p12) was detected in myxoinflammatory fibroblastic sarcoma (MIFS) and MIFS-like tumors [7–11]. Recent RNA sequencing studies have revealed a high frequency of *VGLL3* fusions in hybrid schwannoma-perineurioma; the most common fusion partners include *CHD7*, *CHD9* and *MAMLD1* [12,13].

Finally, *VGLL4* was shown recently to play an important role in prognosis and tumorigenesis in breast and lung cancer [14].

To our knowledge, only a single case of myogenic sarcoma has been recently reported to harbor a *VGLL3* fusion (reported as spindle cell RMS) [15]. We herein characterize a distinct spindle cell rhabdomyosarcoma occurring in adults with predilection for the head and neck, defined by recurrent novel *VGLL3* fusions and characterized by bland morphology, limited rhabdomyogenic differentiation, and indolent clinical behavior.

MATERIAL AND METHODS

The cases were identified from the consultation files of the authors. The tissue specimens were fixed in formalin and processed routinely for histopathology. Due to the consultation nature of the cases, immunohistochemistry (IHC) was performed in different laboratories and the stains applied varied from case to case, based on tissue availability and initial differential diagnostic considerations (details of the staining protocols and antibody sources are available upon request).

Next generation sequencing

For Cases 1 and 2, (Table 1), RNA was isolated from formalin-fixed paraffin embedded (FFPE) tissue sections using RNeasy FFPE Kit of Qiagen (Hilden, Germany) and quantified spectrophotometrically using NanoDrop-1000 (Waltham, United States). Molecular analysis was performed using the TruSight RNA Fusion panel (Illumina, Inc., San Diego, CA, USA) with 500 ng RNA as input according to the manufacturer`s protocol. Libraries were sequenced on a MiSeq (Illumina, Inc., San Diego, CA, USA) with > 3 million reads per case, and sequences were analyzed using the RNA-Seq Alignment workflow, version 2.0.1 (Illumina, Inc., San Diego, CA, USA). The Integrative Genomics Viewer (IGV), version 2.2.13 (Broad Institute, REF) was used for data visualization [16]. Cases 3, 4, and 6 were subjected to targeted RNA sequencing using Illumina RNA Fusion assay as described previously [17]. The fusion in Case 4 was additionally independently confirmed by the Archer panel [18]. Case 5 was identified using the Illumina TruSight RNA PanCancer panel.

RESULTS

Clinical and demographic features

The cohort included five males and one female patient, aged 30 to 71 years (median, 56) (Table 1). The tumors originated in the tongue (n=3), nasopharynx (n=1), oral cavity/ alveolar ridge (n=1), and oropharynx (n=1). Different surgical modalities were the primary treatment in all cases; initially R1-resected cases received re-excision to achieve complete tumor removal, except in Case 3, and 6, which received either nonradical resection or incisional biopsy only. One patient received adjuvant irradiation up to 60 Gy, and another (Case 4) postoperative VAC chemotherapy. At last available follow-up, three patients were alive with no evidence of local recurrence or metastases at 8, 19, and 60 months after treatment. One patient was alive with unknown disease status at 24 months.

Pathological findings

The major findings are summarized in Table 2. The submitting pathologists considered spindle cell RMS (n=2), cellular fibrous histiocytoma (1), rhabdomyoma (1), unclassified spindle cell neoplasm (n=1) and low-grade myofibroblastic sarcoma vs. spindle cell rhabdomyosarcoma (n=1). Second opinion diagnosis was spindle cell RMS (n=3), and unclassified low-grade myogenic sarcoma/neoplasm (n=3). The tumor size ranged from 0.8 to 1.6 cm; all tumors, but one, were <1 cm. The size of Case 1 and 3 was not reliably assessable due to the fragmented nature of the submitted specimens (they measured 2.5 and 4.9 cm in aggregate, respectively). Histologically, five tumors were centered within

skeletal muscle with diffuse infiltration and entrapment of muscle fibers with variable degrees of cellularity (Fig. 1A–D). All tumors displayed bland short spindled and ovoid cells arranged into vague fascicular, diffuse or storiform pattern (Table 2) (Fig. 2A–C). Each of the cases lacked significant nuclear atypia, but rare enlarged hyperchromatic nuclei were observed in one tumor (Fig. 3); mitoses ranged from 1 to 7 per 10 HPFs with >2 mitoses seen in only two tumors. Less cellular tumors showed prominently collagenized stroma (Fig. 2D). The background stroma showed a variable mononuclear and histiocytic inflammatory reaction (Fig. 2, 3). The nasopharyngeal tumor showed a similar growth pattern as seen in most of mesenchymal neoplasms of the sinonasal tract with predominantly polypoid growth beneath intact and focally ulcerated metaplastic respiratory mucosa (Fig. 3A). This case displayed remarkably variable cellularity with cellular areas of ovoid and plump cells similar to other cases, alternating with paucicellular areas composed of slender spindled cells in a manner reminiscent of biphenotypic sinonasal sarcoma (Fig. 3B). However, no entrapped hamartoma-like hyperplastic mucosal glands were noted. Rare tumor cells showed xanthomatous cytoplasmic changes mimicking reactive histiocytes (Fig. 3D). Immunohistochemistry revealed consistent expression of desmin (diffuse in 4 and patchy in two cases; (Fig. 4A–C)) associated with patchy smooth muscle actin expression (4/6; Fig. 4D)), and focal, mostly single cell reactivity for myogenin (5/6; Fig. 4E)) and myoD1 (1/3). Several lineage-specific markers (see Table 2) tested negative including S100 and EMA.

Molecular results

Targeted RNA sequencing revealed in-frame *VGLL3* (exon 2) fusions in all cases. The fusion partner was *TCF12* (exon 16) in three tumors, *EP300* (exon 31) in two and *PPARGC1A* (exon 3) in one tumor (Table 3; Fig 5). VGLL3 is present at the 5’ position of the fusion product.

DISCUSSION

Rhabdomyosarcoma (RMS) is a malignant neoplasm defined by evidence of rhabdomyogenic differentiation, either morphologically (presence of striated muscle differentiation) or immunophenotypically (expression of myogenin and MyoD1 in variable proportions of neoplastic cells) [19]. Besides the classical embryonal and alveolar subtypes, and the controversial pleomorphic adult subtype, spindle cell/sclerosing RMS has recently emerged as a distinct fourth category of RMS; these tumors are notable for their significant clinical, morphologic, immunophenotypic, and molecular-genetic heterogeneity [20–27].

The extent of myogenin and MyoD1 expression is known to vary amongst tumor subtypes, with alveolar RMS showing more diffuse myogenin but less MyoD1, while the embryonal subtype usually expresses more MyoD1 [19]. Likewise, MyoD1-mutated spindle cell RMS displays more extensive MyoD1 expression and limited immunoreactivity for myogenin [19,25]. Next-generation sequencing has facilitated characterization of the genetic landscape of diverse mesenchymal neoplasms, including RMS, and it became evident that variable, often limited, rhabdomyogenic differentiation may be encountered in several non-RMS entities, including biphenotypic sinonasal sarcoma, and ectomesenchymal chondromyxoid tumor amongst others [28–30]. These observations challenge the dogma

that immunohistochemical evidence of rhabdomyogenic differentiation equates with RMS; it is conceivable, in the context of some fusion-associated neoplasms, that this may reflect polyphenotypic differentiation induced by the complex downstream molecular pathways initiated by the fusion transcripts.

Most spindle cell RMS originates in the head and neck and the paratesticular region with a striking predilection for neonates, children, and young adults [20–27]. A significant proportion of them are congenital or infantile and are mostly associated with a favorable outcome and lack or have a limited metastatic potential [20–27]. Recently, several gene fusions have been identified in spindle cell RMS, mostly in infantile age group, including *VGLL2::NCOA2*, *VGLL2::CITED2*, *TEAD1::NCOA2*, *HMGA2::NEGR1, CAV1::MET* and *SRF::NCOA2*, or less commonly intra-osseously, such as *EWSR1/FUS::TFCP2* and *NCOA2::MEIS1* fusions [20–27,31]. In contrast, spindle and sclerosing RMS with *MyoD1* mutations, often occurring in the head and neck, are associated with a highly aggressive clinical course and insensitivity to available RMS chemotherapies [25]. Additionally, a subset of clinically indolent well-differentiated RMS occurring in the deep paraspinal region of newborns and young children were found to harbor recurrent *SRF::FOXO1* and *SRF::NCOA1* fusions [32]. The tumors showed unequivocal histological features of skeletal muscle differentiation and more prominent, albeit heterogeneous, expression of MyoD1 and myogenin [32]. Expression profiling studies showed these tumors to cluster separately from all other rhabdomyogenic entities [32]. Combined, these observations reinforce the value of molecular-based subtyping and risk stratification to guide management decisions in RMS [33].

In this study, we describe six unique head and neck neoplasms characterized by limited rhabdomyogenic immunophenotype associated with recurrent *VGLL3* fusions. All tumors occurred in adults, with a mean age of 56 and strong predilection for males (5: 1) and lingual (50%) location. They predominantly arose at an intramuscular location in the muscle of the oral/ oropharyngeal region with diffusely dissecting growth between muscle fibers. These tumors are uniformly desmin-positive and h-caldesmon-negative. A subset contained rare myogenin-positive cells. Despite their limited rhabdomyoblastic differentiation (lack of histological skeletal muscle features and limited myogenin and MyoD1 expression), it is conceivable, that these tumors represent a distinctive molecular subset in the spectrum of spindle cell RMS. Regrettably, the MyoD1 expression status was not available for three of our cases including the two *EP300::VGLL3* fusion tumors. Notably, the *VGLL3* fusion products identified in four of these tumors are novel and have not been reported previously in any entity. A single tumor with similar histology, but more prominent myogenin and MyoD1 expression was included in a recent series of spindle cell RMS published by Montoya-Cerrillo et al [15]. This tumor (which is similar to our Cases 2 – 6) presented as a submucosal muscle-centered mass in the ventral left mid-tongue of a 36-year-old male, who remained disease-free one year after surgical treatment. RNA sequencing revealed an *EP300::VGLL3* fusion similar to the fusion product detected in two of our cases. The one nasopharyngeal/ sinonasal case in our study was more cellular and based on subtle myogenic features might be considered in the spectrum of biphenotypic sinonasal sarcoma, a recently recognized sinonasal entity known to display variable rhabdomyogenic elements, especially

those cases harboring the *PAX3::NCOA1* fusion [28,29]. However, this tumor lacked the classical *MAML3* fusion characteristic of that entity [28,29].

Taken together, five of our cases and the one reported recently by Montoya-Cerrillo et al [15] shared intramuscular location in head and neck, bland histomorphology, minimal to variable rhabdomyogenic differentiation, *VGLL3* rearrangement, and indolent clinical behavior. Moreover, four of the seven cases were located in the tongue. Based on the limited evidence available to date, these features would appear to support "VGLL3-rearranged myogenic neoplasm" as a distinctive tumor in the spectrum of spindle cell RMS. Notably, the known roles of VGLL3 in the regulation of embryonic skeletal myogenesis might explain the rhabdomyogenic trait seen in these tumors, suggesting relatedness to rhabdomyogenic entities [34,35], Further studies (including comparisons of expression analysis and methylation profiling) are necessary to establish whether these tumors warrant classification as a distinct entity, or represent a molecular subtype of spindle cell RMS. Moreover, the full spectrum of biological, morphologic, and molecular characteristics of these tumors remains to be better delineated. Although limited by the low number of cases, our study suggests an indolent behavior of *VGLL3*-rearranged spindle cell RMS, possibly akin to that of *VGLL2*-rearranged head and neck spindle cell RMS in infants and, hence, are associated with a better outcome and lack of metastatic potential in most cases.

Although most of *VGLL2*-associated infantile spindle cell RMS have been indolent, it is worth noting that a recent study reported aggressive clinical course in four patients, whose tumors showed clear-cut cytological atypia and rhabdoid cell features [36].

In summary, we identified and characterized a distinctive mesenchymal neoplasm with myogenic differentiation and a striking predilection for the head and neck. These tumors occurred in adults and possessed a bland histology, minimal rhabdomyoblastic differentiation, indolent clinical behavior, predilection for males and tongue location, and recurrent *VGLL3* fusions. The full biological spectrum and, hence, the most appropriate therapeutic strategy for this rare, but possible underdiagnosed, neoplasm, remains to be defined. Likewise, the relationship of this entity to other molecular subtypes of spindle cell RMS remains to be fully characterized.

Acknowledgement:

The 1st author thanks Dr. Dieter Krahl (Private Laboratory of Dermatohistopathology, Heidelberg, Germany) for providing clinical details of Case 2.

P50 CA 140146–01 (CRA), P50 CA217694 (CRA), P30 CA008748 (CRA); Panov 2 research program (BCD), Dr. Martin Blackstein research fund (BCD)

REFERENCES

1. Mielcarek M, Gunther S, Kruger M, Braun T. VITO-1, a novel vestigial related protein is predominantly expressed in the skeletal muscle lineage. Gene Expr Patterns 2002; 2:305–310. [PubMed: 12617818]
2. Mielcarek M, Piotrowska I, Schneider A, Gunther S, Braun T. VITO-2, a new SID domain protein, is expressed in the myogenic lineage during early mouse embryonic development. Gene Expr Patterns 2009; 9:129–137. [PubMed: 19118645]

3. Pobbati AV, Chan SW, Lee I, Song H, Hong W. Structural and functional similarity between the Vgll1-TEAD and the YAPTEAD complexes. Structure 2012; 20:1135–1140. [PubMed: 22632831]
4. Pobbati AV, Hong W. Emerging roles of TEAD transcription factors and its coactivators in cancers. Cancer Biol Ther 2013; 14:390–398. [PubMed: 23380592]
5. Zhang Y, Shen H, Withers HG, Yang N, Denson KE, Mussell AL, Truskinovsky A, Fan Q, Gelman IH, Frangou C, Zhang J. VGLL4 Selectively Represses YAP Dependent Gene Induction and Tumorigenic Phenotypes in Breast Cancer. Sci Rep 2017;7:6190 DOI:10.1038/s41598-017-06227-7. [PubMed: 28733631]
6. Alaggio R, Zhang L, Sung YS, Huang SC, Chen CL, Bisogno G, Zin A, Agaram NP, LaQuaglia MP, Wexler LH, Antonescu CR. A Molecular Study of Pediatric Spindle and Sclerosing Rhabdomyosarcoma: Identification of Novel and Recurrent VGLL2-related Fusions in Infantile Cases. Am J Surg Pathol 2016;40:224–35. [PubMed: 26501226]
7. Hallor KH, Sciot R, Staaf J, Heidenblad M, Rydholm A, Bauer HC, Aström K, Domanski HA, Meis JM, Kindblom LG, Panagopoulos I, Mandahl N, Mertens F. Two genetic pathways, t(1;10) and amplification of 3p11–12, in myxoinflammatory fibroblastic sarcoma, haemosiderotic fibrolipomatous tumour, and morphologically similar lesions. J Pathol 2009;217:716–27. [PubMed: 19199331]
8. Hélias-Rodzewicz Z, Pérot G, Chibon F, Ferreira C, Lagarde P, Terrier P, Coindre JM, Aurias A. YAP1 and VGLL3, encoding two cofactors of TEAD transcription factors, are amplified and overexpressed in a subset of soft tissue sarcomas. Genes Chromosomes Cancer 2010;49:1161–71. [PubMed: 20842732]
9. Antonescu CR, Zhang L, Nielsen GP, Rosenberg AE, Dal Cin P, Fletcher CD. Consistent t(1;10) with rearrangements of TGFBR3 and MGEA5 in both myxoinflammatory fibroblastic sarcoma and hemosiderotic fibrolipomatous tumor. Genes Chromosomes Cancer 2011;50:757–64. [PubMed: 21717526]
10. Arbajian E, Hofvander J, Magnusson L, Mertens F. Deep sequencing of myxoinflammatory fibroblastic sarcoma. Genes Chromosomes Cancer 2020;59:309–317. [PubMed: 31898851]
11. Suster D, Michal M, Huang H, Ronen S, Springborn S, Debiec-Rychter M, Billings SD, Goldblum JR, Rubin BP, Michal M, Suster S, Mackinnon AC. Myxoinflammatory fibroblastic sarcoma: an immunohistochemical and molecular genetic study of 73 cases. Mod Pathol 2020;33:2520–2533. [PubMed: 32514165]
12. Dickson BC, Antonescu CR, Demicco EG, Leong DI, Anderson ND, Swanson D, Zhang L, Fletcher CDM, Hornick JL. Hybrid schwannoma-perineurioma frequently harbors VGLL3 rearrangement. Mod Pathol 2021;34:1116–1124. [PubMed: 33649458]
13. Nihous H, Baud J, Azmani R, Michot A, Perret R, Mayeur L, de Pinieux G, Milin S, Angot E, Duquenne S, Geneste D, Lucchesi C, Le Loarer F, Bouvier C. Clinicopathologic and Molecular Study of Hybrid Nerve Sheath Tumors Reveals Their Common Association With Fusions Involving VGLL3. Am J Surg Pathol 2022;46:591–602. [PubMed: 35256555]
14. Zhang W, Gao Y, Li P, Shi Z, Guo T, Li F, Han X, Feng Y, Zheng C, Wang Z, Li F, Chen H, Zhou Z, Zhang L, Ji H. VGLL4 functions as a new tumor suppressor in lung cancer by negatively regulating the YAP-TEAD transcriptional complex. Cell Res 2014;24:331–343. [PubMed: 24458094]
15. Montoya-Cerrillo DM, Diaz-Perez JA, Velez-Torres JM, Montgomery EA, Rosenberg AE. Novel fusion genes in spindle cell rhabdomyosarcoma: The spectrum broadens. Genes Chromosomes Cancer 2021;60:687–694. [PubMed: 34184341]
16. Robinson JT, Thorvaldsdóttir H, Winckler W, Guttman M, Lander ES, Getz G, Mesirov JP. Integrative Genomics Viewer. Nature Biotechnology 2011;29:24–26.
17. Dickson BC, Swanson D. Targeted RNA sequencing: A routine ancillary technique in the diagnosis of bone and soft tissue neoplasms. Genes Chromosomes Cancer 2019;58:75–87. [PubMed: 30350361]
18. Zheng Z, Liebers M, Zhelyazkova B, Cao Y, Panditi D, Lynch KD, Chen J, Robinson HE, Shim HS, Chmielecki J, Pao W, Engelman JA, Iafrate AJ, Le LP. Anchored multiplex PCR for targeted next-generation sequencing. Nat Med 2014;20:1479–84. [PubMed: 25384085]

19. WHO Classification of Tumours Editorial Board. Soft tissue and bone tumours. Lyon (France): International Agency for Research on Cancer 2020. (WHO classification of tumours series, 5th ed. Vol. 3). https://publications.Iarc.fr/588.

20. Mosquera JM, Sboner A, Zhang L, Kitabayashi N, Chen CL, Sung YS, Wexler LH, LaQuaglia MP, Edelman M, Sreekantaiah C, Rubin MA, Antonescu CR. Recurrent NCOA2 gene rearrangements in congenital/infantile spindle cell rhabdomyosarcoma. Genes Chromosomes Cancer 2013;52:538–50. [PubMed: 23463663]

21. Alaggio R, Zhang L, Sung YS, Huang SC, Chen CL, Bisogno G, Zin A, Agaram NP, LaQuaglia MP, Wexler LH, Antonescu CR. A Molecular Study of Pediatric Spindle and Sclerosing Rhabdomyosarcoma: Identification of Novel and Recurrent VGLL2-related Fusions in Infantile Cases. Am J Surg Pathol 2016;40:224–35. [PubMed: 26501226]

22. Le Loarer F, Cleven AHG, Bouvier C, Castex MP, Romagosa C, Moreau A, Salas S, Bonhomme B, Gomez-Brouchet A, Laurent C, Le Guellec S, Audard V, Giraud A, Ramos-Oliver I, Cleton-Jansen AM, Savci-Heijink DC, Kroon HM, Baud J, Pissaloux D, Pierron G, Sherwood A, Coindre JM, Bovée JVMG, Larousserie F, Tirode F. A subset of epithelioid and spindle cell rhabdomyosarcomas is associated with TFCP2 fusions and common ALK upregulation. Mod Pathol 2020;33:404–419. [PubMed: 31383960]

23. Congenital spindle cell rhabdomyosarcoma: An international cooperative analysis. Whittle S, Venkatramani R, Schönstein A, Pack SD, Alaggio R, Vokuhl C, Rudzinski ER, Wulf AL, Zin A, Gruver JR, Arnold MA, Merks JHM, Hettmer S, Koscielniak E, Barr FG, Hawkins DS, Bisogno G, Sparber-Sauer M. Eur J Cancer 2022;168:56–64. [PubMed: 35452896]

24. Owosho AA, Chen S, Kashikar S, Zhang L, Chen CL, Wexler LH, Estilo CL, Huryn JM, Antonescu CR. Clinical and molecular heterogeneity of head and neck spindle cell and sclerosing rhabdomyosarcoma. Oral Oncol 2016;58:e6–e11. [PubMed: 27261172]

25. Agaram NP, LaQuaglia MP, Alaggio R, Zhang L, Fujisawa Y, Ladanyi M, Wexler LH, Antonescu CR. MYOD1-mutant spindle cell and sclerosing rhabdomyosarcoma: an aggressive subtype irrespective of age. A reappraisal for molecular classification and risk stratification. Mod Pathol 2019;32:27–36.

26. Butel T, Karanian M, Pierron G, Orbach D, Ranchere D, Cozic N, Galmiche L, Coulomb A, Corradini N, Lacour B, Proust S, Guerin F, Boutroux H, Rome A, Mansuy L, Vérité C, Defachelles AS, Tirode F, Minard-Colin V. Integrative clinical and biopathology analyses to understand the clinical heterogeneity of infantile rhabdomyosarcoma: A report from the French MMT committee. Cancer Med 2020;9:2698–2709. [PubMed: 32087612]

27. Bisogno G, Minard-Colin V, Arush MB, Daragjati J, Coppadoro B, Gallego S, Alaggio R, Smeulders N, Mudry P, Zin A, Merks JHM, Slater O. Congenital rhabdomyosarcoma: A report from the European paediatric Soft tissue sarcoma Study Group. Pediatr Blood Cancer 2022;69:e29376. [PubMed: 34582098]

28. Huang S-C, Ghossein RA, Bishop JA, et al. Novel PAX3-NCOA1 fusions in biphenotypic sinonasal sarcoma with focal rhabdomyoblastic differentiation. Am J Surg Pathol 2016;40:51–59. 29. [PubMed: 26371783]

29. Andreasen S, Bishop JA, Hellquist H, et al. Biphenotypic sinonasal sarcoma: demographics, clinicopathological characteristics, molecular features, and prognosis of a recently described entity. Virchows Arch 2018;473:615–626. [PubMed: 30109475]

30. Dickson BC, Antonescu CR, Argyris PP, Bilodeau EA, Bullock MJ, Freedman PD, Gnepp DR, Jordan RC, Koutlas IG, Lee CH, Leong I, Merzianu M, Purgina BM, Thompson LDR, Wehrli B, Wright JM, Swanson D, Zhang L, Bishop JA. Ectomesenchymal Chondromyxoid Tumor: A Neoplasm Characterized by Recurrent RREB1-MKL2 Fusions. Am J Surg Pathol 2018;42:1297–1305. [PubMed: 29912715]

31. Agaram NP, Zhang L, Sung YS, Cavalcanti MS, Torrence D, Wexler L, Francis G, Sommerville S, Swanson D, Dickson BC, Suurmeijer AJH, Williamson R, Antonescu CR. Expanding the Spectrum of Intraosseous Rhabdomyosarcoma: Correlation Between 2 Distinct Gene Fusions and Phenotype. Am J Surg Pathol 2019 May;43(5):695–702. [PubMed: 30720533]

32. Karanian M, Pissaloux D, Gomez-Brouchet A, Chevenet C, Le Loarer F, Fernandez C, Minard V, Corradini N, Castex MP, Duc-Gallet A, Blay JY, Tirode F. SRF-FOXO1 and SRF-NCOA1

Fusion Genes Delineate a Distinctive Subset of Well-differentiated Rhabdomyosarcoma. Am J Surg Pathol 2020;44:607–616. [PubMed: 32187044]

33. Arnold MA, Barr FG. Molecular diagnostics in the management of rhabdomyosarcoma. Expert Rev Mol Diagn 2017;17:189–194. [PubMed: 28058850]
34. Chen HH, Mullett SJ, Stewart AF. Vgl-4, a novel member of the vestigial-like family of transcription cofactors, regulates alpha1-adrenergic activation of gene expression in cardiac myocytes. J Biol Chem 2004;279:30800–6. [PubMed: 15140898]
35. Figeac N, Mohamed AD, Sun C, Schönfelder M, Matallanas D, Garcia-Munoz A, Missiaglia E, Collie-Duguid E, De Mello V, Pobbati AV, Pruller J, Jaka O, Harridge SDR, Hong W, Shipley J, Vargesson N, Zammit PS, Wackerhage H. VGLL3 operates via TEAD1, TEAD3 and TEAD4 to influence myogenesis in skeletal muscle. J Cell Sci 2019;132:jcs225946. [PubMed: 31138678]
36. Cyrta J, Gauthier A, Karanian M, Vieira AF, Cardoen L, Jehanno N, Bouvet M, Bouvier C, Komuta M, Le Loarer F, Orbach D, Rome A, Minard-Colin V, Brichard B, Pluchart C, Thebaud E, Renard M, Pannier S, Brisse H, Petit P, Benoist C, Schleiermacher G, Geoerger B, Vincent-Salomon A, Fréneaux P, Pierron G. Infantile Rhabdomyosarcomas With VGLL2 Rearrangement Are Not Always an Indolent Disease: A Study of 4 Aggressive Cases With Clinical, Pathologic, Molecular, and Radiologic Findings. Am J Surg Pathol 2021;45:854–867. [PubMed: 33949344]
37. Gu Z, Gu L, Eils R, Schlesner M, Brors B. circlize Implements and enhances circular visualization in R. Bioinformatics 2014;30:2811–2. [PubMed: 24930139]

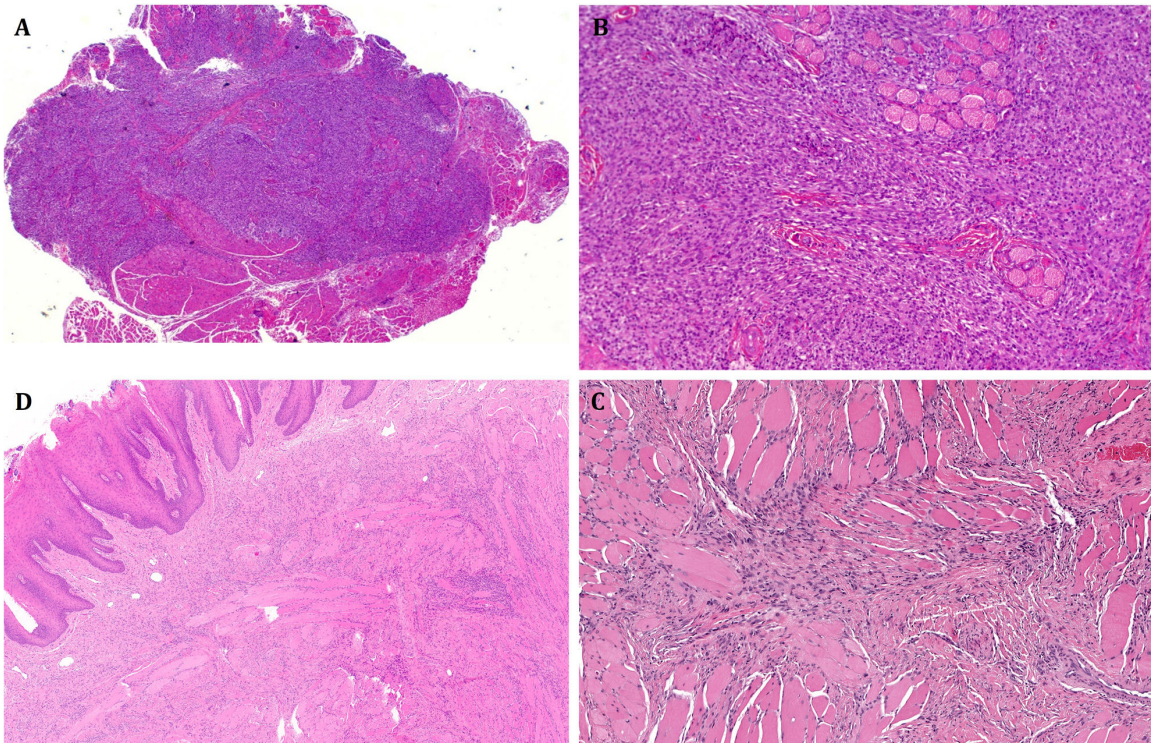

Figure 1.

Representative low-power views of *VGLL3*-rearranged spindle cell RMS showing invasive intramuscular growth with vague lobulation and moderate cellularity (**A**; Case 2), note entrapped skeletal muscle fibers in **B** (Case 2). **C**: This low cellularity tumor was centered within the tongue musculature and showed diffuse infiltration mimicking a reactive fibroblastic lesion (**D**).

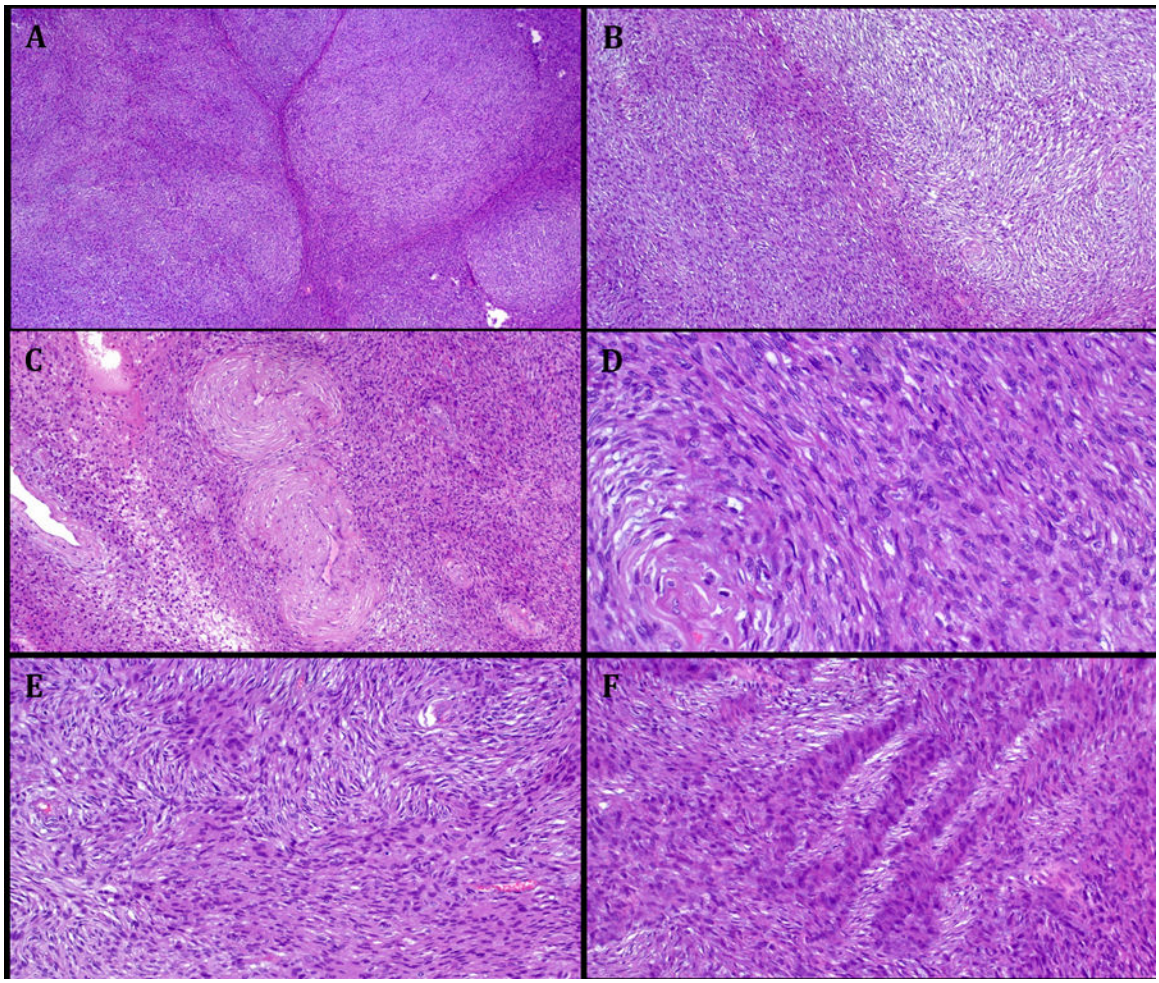

Figure 2.

A: Monomorphic bland ovoid cells with dispersed mononuclear inflammatory cells in the background (Case 3). **B**: Higher magnification of same tumor. **C**: Prominent fibroma-like storiform pattern (Case 5). **D**: Densely collagenized stroma (Case 4).

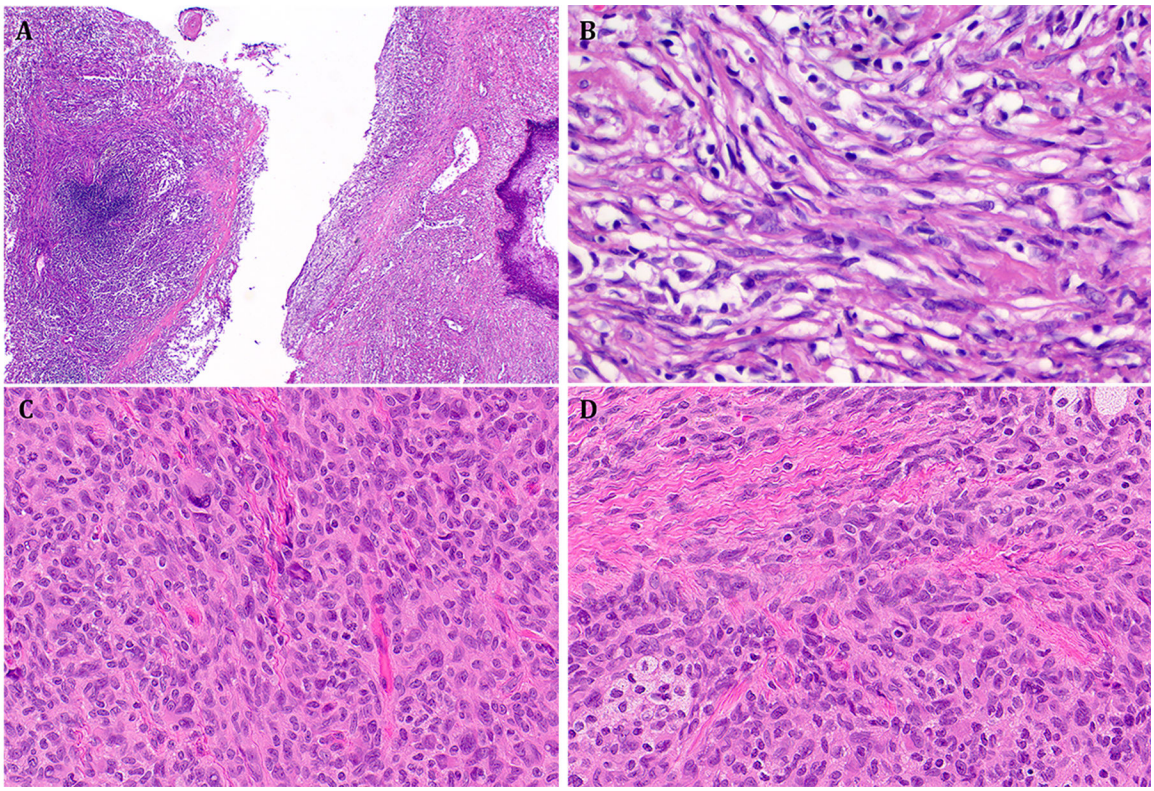

Figure 3.

A: This fragmented nasopharyngeal specimen of Case 1 showed metaplastic squamous epithelium (right) covering variably cellular lesion, note prominent dark-stained lymphoid aggregates on left. **B**: Same tumor showing paucicellular foci of slender spindled cells reminiscent of biphenotypic sinonasal sarcoma. **C**: A few scattered enlarged degenerative-type nuclei were seen in Case 6. **D**: Same tumor showing foci of foamy cell change, reminiscent of histiocyte-rich rhabdomyoblastic tumor.

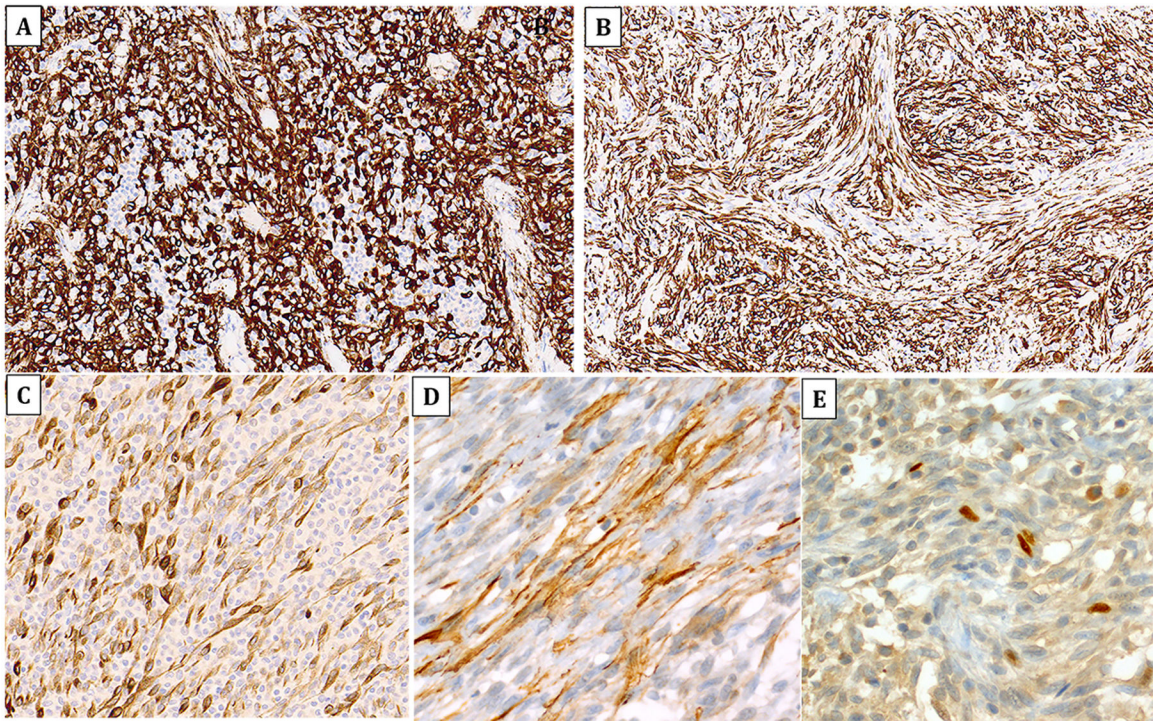

Figure 4.

Immunohistochemistry revealed strong desmin expression in all cases (**A**: ovoid cell areas in Case 6; **B**: spindle cell storiform area in Case 5). **C**: Less diffuse desmin reactivity in Case 3 (note desmin-negative inflammatory cells in the background). **D**: Patchy expression of smooth muscle actin in Case 1. **E**: Very rare cells expressed myogenin (Case 1).

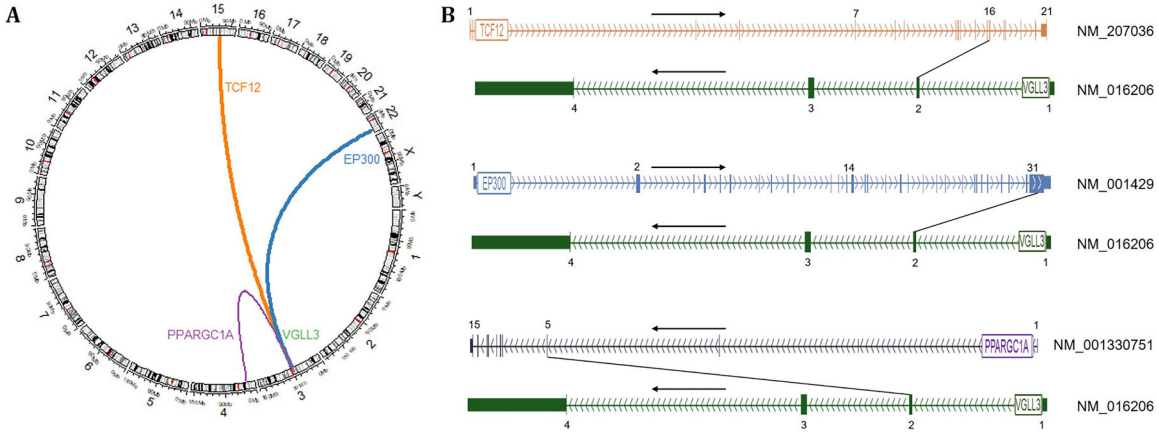

Figure 5.

A: Circos plot depicting *VGLL3* fusions represented by links between cytobands (hg19 genome). Plot generated using R package "circlize" version 0.4.13 (ref. 37). **B**: Schematic of *VGLL3* fusion transcripts annotated by NCBI RefSeq accession numbers. Numbers and black arrows represent exons and directions of transcript, respectively.

Table 1:

Clinicopathological features of VGLL3-rearranged low-grade myogenic neoplasms

No	Age/sex	Site	Tumor epicenter	Size (cm)	Gene fusion	Treatment	Outcome
1	71/F	Nasopharynx	Mucosa/ submucosal	NA *	*TCF12::VGLL3*	Biopsy, then resection 13 month later (Rx), adjuvant irradiation (60 Gy)	NED (60 mo)
2	59/M	Vestibular region 41 – 43, lower jaw	Intramuscular	0.8	*TCF12::VGLL3*	Marginal excision, reexision (R0)	NED (19 mo)
3	30/M	Oropharynx	Intramuscular	NA *	*TCF12::VGLL3*	Piecemeal excision (Rx)	Alive, unknown disease status (24 mo)
4	42/M	Dorsal tongue submucosal	Intramuscular	1.6	*PPARGC1A::VGLL3*	Biopsy followed by partial glossectomy (R0), adjuvant VAC chemotherapy	NED (8 mo)
5	59/M	Tongue	Intramuscular	0.9	*EP300:VGLL3*	Incomplete excision, reexcision (R0)	Recent case
6	54/M	Tongue	Intramuscular	0.8	*EP300:VGLL3*	Incisional biopsy	Recent case

*exact size not assessable due to specimen fragmentation; mo=months; NA=not available; NED=no evidence of disease.

Table 2:

Pathological features of VGLL3-rearranged low-grade myogenic head and neck neoplasms

No	Submitted diagnosis	2nd opinion diagnosis	Tumor borders	Cell morphology	Mitoses/10 HPFs*	Necrosis	Background inflammatory cells/histiocytes	Positive IHC	Negative IHC
1	Cellular fibrous histiocytoma vs NOS	Unclassified low-grade myogenic neoplasm	Infiltrative	Spindled & ovoid	7	Absent	Mild	Desmin, SMA (patchy), CD56, CD68, myogenin (i+)	h-caldesmon, MyoD1, AE1/AE3, S100, SOX10, CD34, MelanA, HMB45, CD117, STAT6, TLE1, EMA
2	Rhabdomyoma	Unclassified low-grade myogenic spindle cell sarcoma	Infiltrative	Spindled & ovoid	1	Absent	Present	Desmin	SMA, MSA, h-caldesmon, myogenin, MyoD1, p63, AE1/AE3, S100, CD34, ALK-D5F3, EMA, STAT6, MUC4
3	spindle cell neoplasm	Unclassified spindle cell sarcoma with partial myogenic differentiation	Infiltrative	Spindled & ovoid	2	Absent	Present	Desmin (patchy), myogenin (i+)	SMA, S100, SOX10, CD34, EMA
4	Low-grade myofibroblastic sarcoma vs Sc-RMS	Variant Sc-RMS	Infiltrative	Spindled & ovoid	1	Absent	Absent	Desmin, SMA (patchy), myogenin (i+), MyoD1 (i+)	MSA, S100, CD34
5	Sc-RMS	Sc-RMS	Infiltrative	Spindled & ovoid	2	Absent	Absent	Desmin, SMA (F), myogenin (F)	S100, panCK, h-caldesmon
6	Sc-RMS	Sc-RMS	Infiltrative	Spindled & ovoid	4	Absent	Mild	Desmin, SMA, MSA, myogenin (i+)	S100, SOX10, CD34, panCK, p63

F=focal; HPF=high-power field; i+=isolated cell positive; IHC=immunohistochemistry; MSA= muscle-specific actin; Sc-RMS=spindle cell rhabdomyosarcoma; SMA=smooth muscle actin.

*The 1 HPF area corresponds to 0.238 mm^2 for Case 1 & 2 and 0.236 mm^2 for Case 3 to 6.

Table 3:

Genes and exons involved in VGLL3-rearranged low-grade myogenic neoplasms

No	Breakpoints gene 1	Breakpoints gene 2
1	*TCF12* (NM_207036.2; exon 16 of 21)	*VGLL3* (NM_016206.4; exon 2 of 4)
2	*TCF12* (NM_207036.2; exon 16 of 21)	*VGLL3* (NM_016206.4; exon 2 of 4)
3	*TCF12* (NM_207036.2; exon 16 of 21	*VGLL3* (NM_016206.4; exon 2 of 4)
4	*PPARGC1A* (NM_001330751.2; exon 5 of 15)	*VGLL3* (NM_016206.4; exon 2 of 4)
5	*EP300* (NM_001429.4; exon 31 of 31)	*VGLL3* (NM_016206.4; exon 2 of 4)
6	*EP300* (NM_001429.4; partial exon 31 of 31)	*VGLL3* (NM_016206.4; partial exon 2 of 4)